Optical and Quantum Electronics **29** *(1997) 923–931*

Spatial characterization of the transversal structure of rotationally symmetric pulsed beams

C. MARTÍNEZ, F. ENCINAS-SANZ, J. SERNA,
P. M. MEJÍAS, R. MARTÍNEZ-HERRERO
Departamento de Óptica, Facultad de Ciencias Físicas,
Universidad Complutense, 28040 Madrid, Spain

Received 25 May; revised 7 July; accepted 8 July 1997

A simple analytical model is proposed to describe the transversal spatial structure of a tridimensional rotationally symmetric pulsed beam. The spatial behaviour of the pulse amplitude is shown to be linked to its (measurable) second- and higher-order intensity moments, namely, beam width, quality parameter and kurtosis. As an illustrative experimental example, this model has been applied to high-quality TEA CO_2 laser pulses.

1. Introduction

A simple bidimensional analytical model was recently proposed [1] for characterizing the transversal spatial structure of a pulsed beam in terms of (measurable) second-order intensity moments [2–6], integrated along the pulse duration. In that model, each spectral component of the field amplitude was expanded in terms of Hermite–Gauss functions, which were assumed to correspond to the empty cavity modes. However, in problems having a large amount of rotational symmetry around the propagation axis, the Laguerre–Gauss (L–G) functions could be more convenient. Since the pulses we analyse in the present paper exhibit this kind of symmetry, we will use Laguerre–Gauss functions for mode calculations.

Thus, in this work we will extend the previous model to realistic rotationally symmetric tridimensional pulsed beams. Moreover, higher-order intensity moments have also been considered. In fact, the behaviour under propagation of the so-called kurtosis parameter (integrated along the pulse length) has been investigated both analytically and experimentally. In the next section the overall intensity moments are defined for tridimensional (3-D) pulsed beams. In Section 3, after applying the analytical model to describe a laser pulse, a number of equations are inferred which link the transversal spatial structure of the beam with the usual second-order intensity moments. To illustrate the above model, these equations are applied in Section 4 to pulses emitted by a TEA CO_2 laser device. In Section 5, it is shown that the behaviour (under free propagation) of the overall kurtosis parameter of the pulsed beam should be taken into account when analysing the mode content according to our model. Finally the main conclusions are summarized in Section 6.

0306–8919

2. Definitions

Let us consider a light beam whose amplitude at plane $z = 0$ is denoted by the function $g(\mathbf{r}, t)$. It is useful to introduce the following Fourier transforms:

$$\psi(\mathbf{r}, \omega) = \int g(\mathbf{r}, t) \exp(-\mathrm{i}\omega t)\ \mathrm{d}t \tag{1}$$

$$G(\boldsymbol{\eta}, \omega) = \int \psi(\mathbf{r}, \omega) \exp(-\mathrm{i}k\boldsymbol{\eta}\mathbf{r})\ \mathrm{d}\mathbf{r} \tag{2}$$

where $\mathbf{r} = (x, y)$, $\boldsymbol{\eta} = (u, v)$, u and v representing angles of propagation (without taking the evanescent waves into account), ω is the temporal frequency, $k = \omega/c$, and c is the speed of light. It follows from Equations 1 and 2 that the squared moduli of ψ and G are related, respectively, to the intensity at $\mathbf{r}$ and to the radiant intensity along the direction $\boldsymbol{\eta}$, associated to the spectral component ω. The overall second-order intensity moments can accordingly be written in the common way, e.g., the squared beam width along the x-axis takes the form

$$\langle x^2 \rangle = \frac{1}{\psi_0} \int x^2 |\psi(\mathbf{r}, \omega)|^2\ \mathrm{d}\mathbf{r}\ \mathrm{d}\omega \tag{3}$$

the associated squared far-field divergence is given by

$$\langle u^2 \rangle = \frac{1}{G_0} \int u^2 |G(\boldsymbol{\eta}, \omega)|^2\ \mathrm{d}\boldsymbol{\eta}\ \mathrm{d}\omega \tag{4}$$

and the crossed parameter $\langle xu \rangle$ (related to the position of the waist plane along the x-axis) is inferred from the formula

$$\langle xu \rangle = \frac{c}{2\mathrm{i}\omega_0 \psi_0} \int x[(\psi^\star)'\psi - \psi^\star \psi']\ \mathrm{d}\mathbf{r}\ \mathrm{d}\omega \tag{5}$$

where $\psi_0 = \int |\psi(\mathbf{r}, \omega)|^2\ \mathrm{d}\mathbf{r}\ \mathrm{d}\omega$, $G_0 = \int |G(\boldsymbol{\eta}, \omega)|^2\ \mathrm{d}\boldsymbol{\eta}\ \mathrm{d}\omega$, the prime denotes derivation with respect to x, and ω_0 is the mean frequency. Similar relations hold for the y-components. It should be understood that the pulsed beam is averaged over the pulse transit time across the plane $z = 0$. For the sake of simplicity, we will assume in the following that $\langle x \rangle = \langle y \rangle = \langle u \rangle = \langle v \rangle = 0$. We will also consider that the fields we analyse are spectrally well-centred and locally quasimonochromatic (SCLQ) beams [7], for which the overall spatial second-order moments follow the *ABCD* law (within the paraxial approach). In particular, the light pulses generated by TEA CO_2 lasers we handle in the experiments belong to this class of fields.

Finally, the beam quality parameter along the x-axis, Q_x, can be defined as follows:

$$Q_x = \langle x^2 \rangle \langle u^2 \rangle - \langle xu \rangle^2 \tag{6}$$

where $\langle xu \rangle = 0$ at the waist plane. Note that SCLQ beams fulfil [7]

$$\langle x^2 \rangle \langle u^2 \rangle \geq \frac{c^2}{4\omega_0^2} \tag{7}$$

and analogously for the orthogonal y-axis. In Equation 7 the equality is reached by beams whose transversal profile is Gaussian. The above expression is identical to the one that applies to CW laser beams.

3. Theory

Let us now consider a pulsed beam at its waist plane. We assume here that the conditions $\langle xu \rangle = 0$ and $\langle yv \rangle = 0$ are fulfilled at the same plane (waist plane). We then write each spectral component of the field, $\psi(\mathbf{r}, \omega)$, in the form

$$\psi(\mathbf{r}, \omega) = \sum_{n=0}^{N} \alpha_n f_n(\mathbf{r}, \omega) \tag{8}$$

where f_n, $n = 0 \ldots N$ represent the laser modes. In Equation 8 we associate the term 'modes' to definite spatial structures of the laser field, which resonate within the loaded cavity. Accordingly, each value of index n refers to a particular spatial structure. It should be noted that the spatial structure will be essentially the same for any axial mode frequency within the linewidth of the laser oscillator. The presence of different f_n would then imply the existence of different transversal modes. In addition, since different modes involve different sets of transverse mode resonance frequencies, we have

$$\int f_n^{\star}(\mathbf{r}, \omega) f_m(\mathbf{r}, \omega) \, \mathrm{d}\omega = 0, \qquad n \neq m \tag{9}$$

Let us now introduce the Laguerre–Gauss (L–G) functions, $u_{pm}(\mathbf{r}) = u_{pm}(r, \theta)$. Keeping in mind the spatial symmetry of the pulse profiles we handle in this paper (either analytically or experimentally), the functions $u_{pm}(r, \theta)$ can be assumed to correspond to the empty cavity modes, i.e.,

$$u_{pm}(r, \theta) = \beta_{pm} (\gamma r)^m L_p^m (\gamma^2 r^2) \exp(-\gamma^2 r^2/2) \exp(\mathrm{i} m \theta) \tag{10}$$

where β_{pm} is a constant, L_p^m denotes the Laguerre polynomial and γ is a constant which is determined from the geometry of the resonator, namely [8],

$$\gamma^{-1} = \left(\frac{L}{k}\right)^{1/2} \left[\frac{g_1 g_2 (1 - g_1 g_2)}{(g_1 + g_2 - 2 g_1 g_2)^2}\right]^{1/4} \tag{11}$$

where L is the length of the laser cavity, and $g_1 = 1 - L/R_1$ and $g_2 = 1 - L/R_2$ are the resonator g parameters, R_1 and R_2 being the radii of curvature of the mirrors. Taking this into account, we can write the pulse amplitude, $\psi(\mathbf{r}, \omega)$, of the loaded cavity in terms of the empty-cavity modes as follows:

$$\psi(r, \theta, \omega) = \sum_p \sum_m B_{pm}(\omega) u_{pm}(r, \theta), \quad m \leq p \tag{12}$$

where

$$B_{pm}(\omega) = \int \int \psi(r, \theta, \omega) u_{pm}(r, \theta) \; r \, \mathrm{d}r \, \mathrm{d}\theta \tag{13}$$

If the pulse amplitude exhibits a rotationally symmetric behaviour, $\psi(r, \theta, \omega) = \psi(r, \omega)$, and Equation 12 reduces to

$$\psi(r, \omega) = \sum_p B_{p0}(\omega) u_{p0}(r) \tag{14}$$

where

$$B_{p0}(\omega) = \int \int \psi(r, \omega) u_{p0}(r) \; r \, \mathrm{d}r \, \mathrm{d}\theta \tag{15}$$

and

$$u_{p0}(r) = \beta_{p0} L_p^0(\gamma^2 r^2) \exp(-\gamma^2 r^2/2) \tag{16}$$

From the recurrence properties of the L–G functions and their derivatives [9], we get in an analogous way to that used in [10] the following equations

$$2\gamma^2 \langle x^2 \rangle = \sum_p (2p+1) R_{pp} - 2 \sum_p (p+1)\ \mathrm{Re}(R_{p,p+1}) \tag{17}$$

$$4k^2 Q_x = \left[\sum_p (2p+1) R_{pp} \right]^2 - 4 \left| \sum_p (p+1) R_{p,p+1} \right|^2 \tag{18}$$

$$k \langle xu \rangle = - \sum_p (p+1)\ \mathrm{Im}(R_{p,p+1}) \tag{19}$$

with

$$\sum_p R_{pp} = 1 \tag{20}$$

where

$$R_{pq} = \frac{c_{pq}}{P} = \frac{1}{P} \int B_{p0}^{\star}(\omega) B_{q0}(\omega)\ \mathrm{d}\omega \tag{21}$$

and

$$P = \sum_p c_{pp} \tag{22}$$

is proportional to the total energy per pulse. Similar relations hold for the second-order moments $\langle y^2 \rangle$, $\langle yv \rangle$ and for $Q_y = \langle y^2 \rangle \langle v^2 \rangle - \langle yv \rangle^2$. Note that (see Equation 21)

$$|R_{pq}|^2 \leq R_{pp} R_{qq} \tag{23}$$

Using the fact that $\langle xu \rangle = 0$ at the waist plane, Equation 19 becomes

$$\sum_p (p+1)\ \mathrm{Im}(R_{p,p+1}) = 0 \tag{24}$$

and we have

$$4k^2 Q_x = \left[\sum_p (2p+1) R_{pp} \right]^2 - 4 \left\{ \sum_p (p+1)\ \mathrm{Re}(R_{p,p+1}) \right\}^2 \tag{25}$$

Let us now introduce two parameters, namely,

$$s \equiv 2\gamma^2 \langle x^2 \rangle \tag{26}$$

$$t \equiv 2 \sum_p (p+1)\ \mathrm{Re}(R_{p,p+1}) \tag{27}$$

From the application of Equations 17 and 25–27 it follows that

$$s + t = \sum_p (2p+1) R_{pp} \tag{28}$$

and

$$t = \frac{4k^2 Q_x - s^2}{2s} \tag{29}$$

Note that $\langle x^2 \rangle$ and Q_x can be directly obtained from the experiment. Parameters s and t should then be considered as measurable quantities. In conclusion, we have that any rotationally symmetric pulsed beam (as given by Equation 14) must fulfil at the waist plane the following four equations:

$$s + t = \sum_p (2p + 1) R_{pp} \tag{30}$$

$$t/2 = \sum_p (p + 1)\ \mathrm{Re}(R_{p,p+1}) \tag{31}$$

$$0 = \sum_p (p + 1)\ \mathrm{Im}(R_{p,p+1}) \tag{32}$$

$$1 = \sum_p R_{pp} \tag{33}$$

These equations give the relationship between the transversal spatial structure of the pulsed beam and the second-order intensity moments. They are the equivalent counterpart to the expressions we obtained in [1] for the bidimensional case, in which Hermite–Gauss (H–G) functions were used. The main difference with the previous case arises from Equation 31: if $t \neq 0$, Equation 14 should then contain at least two L–G functions, which differ by *one* order. The importance of this fact will become clear in the next section. As in [1], coefficients R_{pp} can be understood as the relative contribution (weight) of each (squared) L–G function in the expansion (14). In addition, Equation 32 comes from the fact that the beam is evaluated at the waist plane. Equation 33 represents a normalization condition.

Note finally that the left-hand side of Equations 30 and 31 can be inferred from the experimental data. In general, the above four equations (30–33) are not enough to determine all the coefficients R_{pq}. This constitutes a limitation of the model regarding the possibility of getting the detailed spatial structure of the pulsed beam from the measurement of the parameters $\langle x^2 \rangle$ and Q_x. Nevertheless, supplementary hypothesis about the behaviour of the modes can overcome this difficulty. For example, in certain cases of interest, the contribution of the higher-order Laguerre–Gauss functions can be assumed small enough to be neglected, as occurs in the example analysed in the next section.

4. Application to TEA CO_2 laser pulses

To illustrate how the mode content can be inferred from Equations 30–33, we will consider in the following the values of the parameters s and t measured (along the x-direction) at the output of a TEA CO_2 laser device. We will use in the calculations the experimental data reported in [1] (see Fig. 1). The ensemble pyroelectric camera (Spiricon PYROCAM I) with laser beam analyser (Spiricon LBA-100A) provides the (squared) beam width (integrated along the complete pulse duration) at different planes after a lens (focal length 500 mm). Pulse energy is nearly 1 J and the pulses last about 100 ns. The laser cavity is a half-symmetric resonator, in which the distance between the curved mirror (radius 10 m)

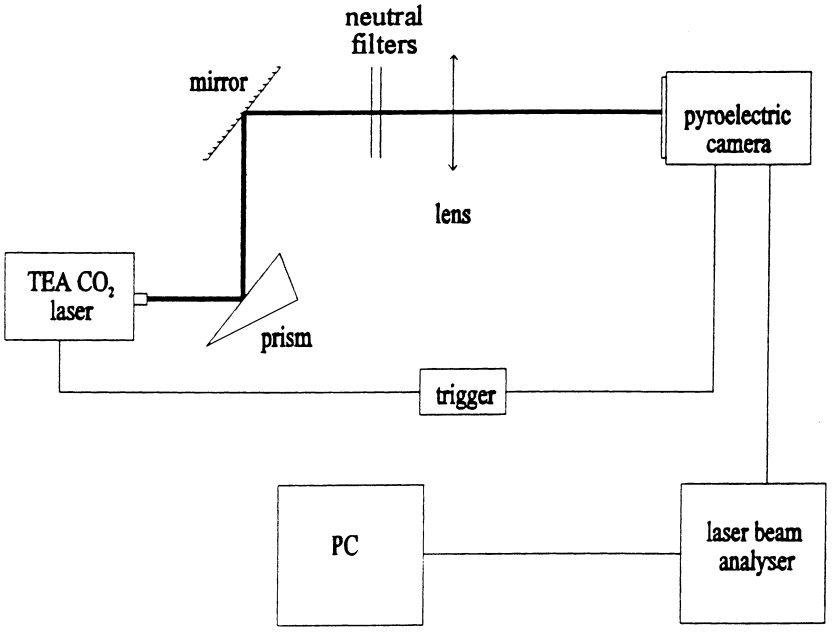

Figure 1 Experimental setup used to measure parameters *s* and *t*.

and the planar (output) mirror is 103 cm. In addition, we have placed an intracavity diaphragm (diameter = 10 mm) close to the curved mirror to increase the beam quality.

We have chosen this kind of beam because of the rotationally symmetric behaviour of their intensity profiles. Also note that the adjustable aperture inside the cavity has circular symmetry.

The presence of multiple modes can be tested from the measurement of the so-called mode beats generated by heterodyne interference effects at the different frequencies between the modes. In the case we are analysing, it was shown [1] the existence of only one mode, namely, f_a. From the experimental data given in [1], we have $\gamma = 0.44\,\text{mm}^{-1}$, $s = 1.33$ and $t = -0.26$. Moreover, since the beam quality products $4k^2Q_x$ and $4k^2Q_y$ are nearly 1, the spatial structure of this mode should be close to the pure rotationally symmetric Gaussian profile. Some difference, however, should exist between such mode and the function u_{00}, because t differs from zero. But, as was pointed out before, this implies that this mode should involve at least the first-order L–G function $u_{10}(r)$ (*cf.* Equation 31). Accordingly, we can consider that the pulse amplitude (as given by Equation 14) can be written in terms of the L–G functions u_{00} and u_{10} as follows:

$$f_a(r,\omega) = B_{00}^{(a)}(\omega)u_{00}(r) + B_{10}^{(a)}(\omega)u_{10}(r) \tag{34}$$

where now

$$\frac{1}{P_a}\int |B_{p0}^{(a)}|^2 \,\mathrm{d}\omega = R_{pp}^{(a)} \tag{35}$$

and

$$P_a = \int |f_a|^2 \, r \,\mathrm{d}r \,\mathrm{d}\theta \,\mathrm{d}\omega \tag{36}$$

From Equations 30 and 31 it then follows that

$$1.07 = R_{00}^{(a)} + 3R_{11}^{(a)} \tag{37}$$

and

$$1 = R_{00}^{(a)} + R_{11}^{(a)} \tag{38}$$

which implies

$$R_{00}^{(a)} = 0.965 \tag{39}$$

$$R_{11}^{(a)} = 0.035 \tag{40}$$

We then have that the spatial structure would be composed of 96.5% of the zero-order L–G function, $u_{00}(r)$, and of 3.5% of the first-order L–G function, $u_{10}(r)$. It is clear from the above that the presence of the active medium slightly distorts the spatial profile of the beam, which would be purely Gaussian for the empty cavity. In comparison with the expressions obtained when H–G functions are used, Equations 39 and 40 enable us to determine the *exact* contribution of each L–G function to the laser mode. It should be noted that the experimental data from which the values of R_{00} and R_{11} have been inferred are the beam width and the beam quality parameter only.

5. Influence of the kurtosis behaviour in the mode expansions

As is well known, the degree of flatness (or sharpness) of any beam intensity distribution can be represented by the so-called kurtosis parameter [11], defined in terms of higher-order intensity moments. Thus, for example, the kurtosis, K_x, along the x-axis is given by the expression

$$K_x = \frac{\langle x^4 \rangle}{\langle x^2 \rangle^2} \tag{41}$$

and K_y is defined in a similar form. In an analogous way to that used in [7], it can be shown that the overall spatial third- and fourth-order moments of SCLQ beams follow the same *ABCD* law that applies for CW beams. Consequently, the kurtosis propagates according to this law. In particular, for the pulsed beams we have considered in the previous section, the behaviour of K_x (integrated along the pulse duration) is shown in Fig. 2. This figure plots the kurtosis of the output beam under free propagation. At each plane z, three values of K_x (which correspond to three emitted pulses) are registered. Dispersion of the experimental data comes from the influence of the tails of the beam profile in offset and cutoff corrections. This effect is particularly increased when fourth- or higher-order intensity moments are evaluated. In spite of this trouble, we can clearly distinguish in the global shape of the experimental points plotted in Fig. 2 one maximum and one minimum of K_x (a similar result was also reported in [12] and [13], concerning industrial CW CO_2 lasers).

Recently [14], a general classification scheme of light beams was given in terms of the kurtosis behaviour under free propagation. According to this scheme, the output beam of our TEA CO_2 laser device fits the type IV. But, for those beams belonging to type IV either m or q must differ from zero [14], where

$$m \equiv \langle u^4 \rangle \langle xu \rangle - \langle u^2 \rangle \langle xu^3 \rangle \tag{42}$$

and

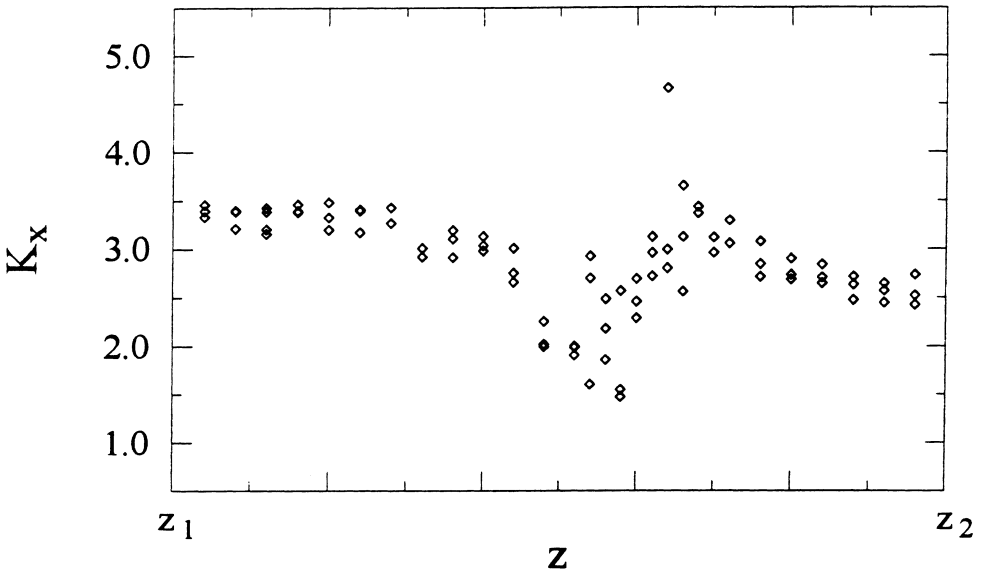

Figure 2 Evolution of the kurtosis parameter, K_x, of the output pulsed beam (integrated along the pulse length) under free propagation. In the figure $(z_2 - z_1) = 500$ mm.

$$q \equiv 3\langle xu^3\rangle\langle x^2\rangle - 3\langle x^3u\rangle\langle u^2\rangle \tag{43}$$

It can be shown that the global pulse amplitude given by Equation 34 fulfils $m = q = 0$. This implies that at least a third L–G function (namely, $u_{20}(r)$) should also be added to the mode expansion in order that the resulting pulsed beam can belong to the type IV. Accordingly, by writing f_a in the form

$$f_a(r,\omega) = B_{00}^{(a)}(\omega)u_{00}(r) + B_{10}^{(a)}(\omega)u_{10}(r) + B_{20}^{(a)}(\omega)u_{20}(r) \tag{44}$$

where

$$\frac{1}{P_a}\int |B_{20}^{(a)}|^2 \, \mathrm{d}\omega = R_{22}^{(a)} \tag{45}$$

it is easy to see that Equations 37 and 38 now become

$$1.07 = R_{00}^{(a)} + 3R_{11}^{(a)} + 5R_{22}^{(a)} \tag{46}$$

$$1 = R_{00}^{(a)} + R_{11}^{(a)} + R_{22}^{(a)} \tag{47}$$

and we then obtain at once

$$R_{00}^{(a)} > 0.948 \tag{48}$$

$$R_{11}^{(a)} < 0.035 \tag{49}$$

$$R_{22}^{(a)} < 0.017 \tag{50}$$

which is similar to the result we got in the bidimensional case (see [1]) using a bidimensional H–G expansion without taking the behaviour of the kurtosis parameter into account. With respect to the values of the coefficients $R_{00}^{(a)}$ and $R_{11}^{(a)}$ found before (Equations 39 and 40), it is immediately seen that the differences are quite small: the predicted spatial structures of the pulse are nearly the same in both approaches.

6. Conclusions

The spatial structure of a tridimensional rotationally symmetric pulsed beam has been shown to be linked to its second- and higher-order intensity moments integrated along the pulse length. In our model each spectral component of the pulse amplitude has been written in terms of L–G functions. A number of equations were found that enable us to infer the relative contribution of each L–G function from the values of the width, the quality parameter and the kurtosis of the pulsed beam. The mode content has been experimentally investigated for the special case of high-quality pulses emitted by a TEA CO_2 laser device. For this kind of pulses, the spatial structure would be composed of nearly 95% of the zero-order L–G function, $u_{00}(r)$, and it should also involve at least the first- and the second-order L–G functions, $u_{10}(r)$ and $u_{20}(r)$, whose contributions do not exceed 3.5% and 1.5%, respectively.

Acknowledgements

The research work leading to this paper has been supported by the Comisión Interministerial de Ciencia y Tecnología of Spain under Project TAP96-2333-E, within the framework of the EU-1269 Project.

References

1. C. MARTÍNEZ, F. ENCINAS-SANZ, J. SERNA, P. M. MEJÍAS and R. MARTÍNEZ-HERRERO, *Proc. SPIE* **2870** (1996) 233.
2. S. LAVI, R. PROCHASKA and E. KEREN, *Appl. Opt.* **27** (1988) 3696.
3. M. J. BASTIAANS, *Optik* **82** (1989) 173.
4. A. E. SIEGMAN, *Proc. SPIE* **1224** (1990) 2.
5. J. SERNA, R. MARTÍNEZ-HERRERO and P. M. MEJÍAS, *J. Opt. Soc. Am. A* **8** (1991) 1096.
6. H. WEBER, *Opt. Quantum Electron.* **24** (1992) 1027.
7. P. M. MEJÍAS and R. MARTÍNEZ-HERRERO, *Opt. Lett.* **20** (1995) 660.
8. A. E. SIEGMAN, *Lasers* (University Science Books, Mill Valley, CA, 1986) Chs. 16 and 19.
9. I. S. GRADSHTEIN and I. M. RYZHIK, *Table of Integrals, Series and Products* (Academic Press, Inc., San Diego, 1980) 4th edn.
10. R. MARTÍNEZ-HERRERO and P. M. MEJÍAS, *Opt. Commun.* **94** (1992) 197.
11. G. PIQUERO, P. M. MEJÍAS and R. MARTÍNEZ-HERRERO, *Opt. Commun.* **107** (1994) 179.
12. P. LOOSEN, K. DU, C. MAIER, O. MÄRTEN and M. SCHOLL, in *Laser Beam Characterization*, edited by P. M. Mejías, H. Weber, R. Martínez-Herrero and A. González-Ureña (SEDO, Madrid, 1993) pp. 249–262.
13. G. HERZIGER, M. SCHOLL and P. LOOSEN, in *Laser Beam Characterization*, edited by H. Weber, N. Reng, J. Lüdtke and P. M. Mejías (FLI, Berlin, 1994) pp. 304–319.
14. R. MARTÍNEZ-HERRERO, G. PIQUERO and P. M. MEJÍAS, *Opt. Commun.* **115** (1995) 225.